

# Impact of Mixing Parameters on Homogenization of Borax Solution and Nucleation Rate in Dual Radial Impeller Crystallizer

A. Kaćunić, M. Ćosić, N. Kuzmanić

**Abstract**—Interaction between mixing and crystallization is often ignored despite the fact that it affects almost every aspect of the operation including nucleation, growth, and maintenance of the crystal slurry. This is especially pronounced in multiple impeller systems where flow complexity is increased. By choosing proper mixing parameters, what closely depends on the knowledge of the hydrodynamics in a mixing vessel, the process of batch cooling crystallization may considerably be improved. The values that render useful information when making this choice are mixing time and power consumption. The predominant motivation for this work was to investigate the extent to which radial dual impeller configuration influences mixing time, power consumption and consequently the values of metastable zone width and nucleation rate. In this research, crystallization of borax was conducted in a 15 dm<sup>3</sup> baffled batch cooling crystallizer with an aspect ratio (H/T) of 1.3. Mixing was performed using two straight blade turbines (4-SBT) mounted on the same shaft that generated radial fluid flow. Experiments were conducted at different values of N/NJS ratio (impeller speed/minimum impeller speed for complete suspension), D/T ratio (impeller diameter/crystallizer diameter), c/D ratio (lower impeller off-bottom clearance/impeller diameter), and s/D ratio (spacing between impellers/impeller diameter). Mother liquor was saturated at 30°C and was cooled at the rate of 6°C/h. Its concentration was monitored in line by Na-ion selective electrode. From the values of supersaturation that was monitored continuously over process time, it was possible to determine the metastable zone width and subsequently the nucleation rate using the Mersmann's nucleation criterion. For all applied dual impeller configurations, the mixing time was determined by potentiometric method using a pulse technique, while the power consumption was determined using a torque meter produced by Himmelstein & Co. Results obtained in this investigation show that dual impeller configuration significantly influences the values of mixing time, power consumption as well as the metastable zone width and nucleation rate. A special attention should be addressed to the impeller spacing considering the flow interaction that could be more or less pronounced depending on the spacing value.

**Keywords**—Dual impeller crystallizer, mixing time, power consumption, metastable zone width, nucleation rate.

## I. INTRODUCTION

CRYSTALLIZATION is a valuable separation and purification technique in many domains, such as

A. Kacunic, M. Ćosić and N. Kuzmanić are with the Faculty of Chemistry and Technology, Department of Chemical Engineering, University of Split (phone: 00385 21329420; e-mail: akacunic@ktf-split.hr, akrap@ktf-split.hr, kuzmanic@ktf-split.hr).

This research has been financially supported by the Croatian Science Foundation and is a part of the HETMIX project (2014.-2018.).

chemical, pharmaceutical and food industries. If crystallization is conducted in a stirred vessel, mixing can affect crystallization kinetics and consequently the properties of the product, including crystal size distribution, purity and morphology. Although it has been empirically known that impeller and crystallizer geometry have a considerable effect on the product, this problem has rarely been quantitatively investigated [1]–[3] and in many cases crystallization is carried out without any optimization of the hydrodynamic conditions [4], [5].

In a mixing vessel (which crystallizer in this research is), the flow pattern generated by impellers is a strong function of mixing characteristics such as type of the impeller, geometry of the impeller, presence or absence of the baffles, geometry of the reactor and rheological properties of the fluid [6]. In order to obtain a desired product, each crystallizer, regardless of its size, requires a proper selection of the mixing characteristics.

To what degree a certain system is mixed, can be assessed by several parameters, with mixing time as the most important one [7]. It is defined as the time necessary to achieve a given homogeneity from the non-equilibrium level after a small volume of tracer has been injected into the mixing vessel [8]. Over the past decades, numerous studies on this subject have been published [9]–[15]. The majority of which has been conducted in a single impeller system, which is adequate for small scale processes. However, for plant scale, a multiple impeller system with an aspect ratio higher than one is a more desirable option. In these systems, mixing time has rarely been investigated and is still an open issue.

The aim of this work was to investigate how dual radial impeller configuration influences mixing time and power consumption in a batch cooling crystallizer. The effect of the same configurations on the nucleation rate of borax decahydrate (in a batch cooling crystallizer was tested as well.

Boron compounds, including borax decahydrate, have a wide range of applications almost in all manufacturing areas, except food [16]. The production of borax crystals of a certain composition and crystal size distribution is dependent on crystallization kinetics which in turn is dependent on fluid dynamics of the suspension.

This study gives a contribution to establishing an efficient dual impeller configuration for the process of batch cooling crystallization of borax.

## II. EXPERIMENTAL PROCEDURES

Experiments were performed in a laboratory-scale ( $15 \text{ dm}^3$ ) stirred batch cooling crystallizer (Fig. 1). The crystallizer was a cylindrical flat bottom vessel with an internal diameter ( $d_T$ ) of 0.24 m and liquid height to tank diameter ( $H/d_T$ ) of 1.3. This aspect ratio enabled an investigation of a dual impeller system. Both impellers were radial straight blade turbines (SBT), mounted on the same shaft. The vessel was equipped with four baffles placed at  $90^\circ$  around the vessel periphery.

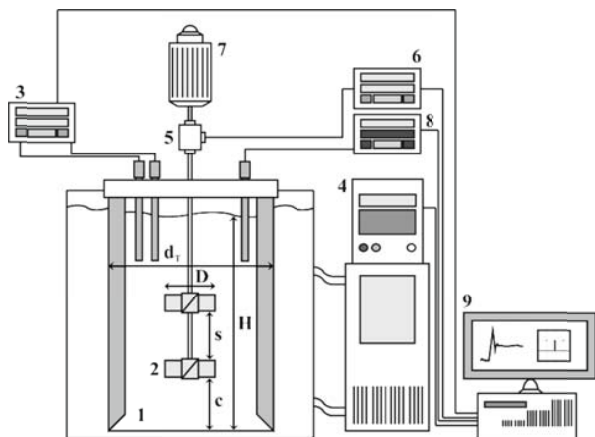


Fig. 1 Schematic illustration of the apparatus (1: crystallizer, 2: impeller, 3: Na-ISE concentration measurement system, 4: thermostat, 5: torque sensor, 6: torque measurement system, 7: electromotor, 8: temperature measurement system, 9: computer)

All measurements (excluding the ones which relate to the investigation of an influence of  $N/N_{JS}$ ) were conducted at the critical impeller speed which ensured the state of complete suspension -  $N_{JS}$ . The value of this impeller speed was determined for each tested configuration, using a visual  $0.9H$  method according to [17]. The method defines  $N_{JS}$  as the speed at which the slurry height reaches 0.9 of the total liquid height. It should be noted that at the same time, at all examined configurations, Zwitering's "one second criterion" was met [18].

### A. Mixing Time and Power Consumption Measurements

In this research, mixing time -  $t_{95}$  was defined as the time needed for a concentration to reach and remain within 5% of the final value [19]. It was measured by potentiometric method using a pulse technique. The moment of the tracer injection was taken as an initial point of measurement of the mixing time. The point where the signal remained almost constant, that is where the normalized terminal potentiometric signal was within  $\pm 5\%$ , was taken as a truncation point of the measurement. Measurements were conducted in the same reactor, shown in Fig. 1. Sodium chloride solution ( $10 \text{ cm}^3$ ,  $2 \text{ mol dm}^{-3}$ ) was used as a tracer. Distilled water was used as a continuous phase, since its physical properties were almost identical to the ones of saturated solution of borax. The tracer was injected with a syringe approximately 1 cm below the surface, mid-way between the adjacent baffles and at  $0.5 R$ ,

where  $R$  is the radius of the vessel. An addition of the tracer did not alter the rheological properties of the continuous phase.

The change in potential, caused by the tracer, was measured by the Na-ISE placed symmetrically to the injection point with respect to the shaft, at position  $0.86 H$  from the tank bottom. In preliminary studies, the Na-ISE was checked for linearity of its response, which was found to be very good. Data was continuously monitored using an appropriate application. To confirm the values of the mixing time obtained, all measurements were repeated at least five times. The reproducibility of the measurement was within four percent. In this research, mixing time is presented in its dimensionless form - as an  $N \cdot t_{95}$  value, where  $N$  is the impeller speed.

Power consumption was calculated from the values of torque measured by a torque meter produced by Himmelstein & Co.

### B. Batch Cooling Crystallization of Borax Decahydrate

Saturated borax solution was prepared by dissolving 99.9 % pure borax decahydrate in excess regarding the solubility data (Eti Maden Isletmeleri, Turkey) in ultrapure water ( $\kappa=0.054 \mu\text{S cm}^{-1}$ ) [20]–[25] at  $30^\circ\text{C}$ . In order to remove residual salt and any possible impurities, the solution was filtered through a cake of diatomaceous earth by vacuum filtration. Thereafter, prepared saturated solution was cooled at constant cooling rate of  $6^\circ\text{C h}^{-1}$ . Temperature control was accomplished by a programmable thermostatic bath (Medingen TC 250) and an appropriate data acquisition system. During the process, concentration change of borax solution was monitored in line using the Na-ion selective electrode (Na-ISE).

## III. RESULTS AND DISCUSSION

The first part of the research was related to the investigation of mixing time. It was measured for different operating conditions, impeller speed -  $N/N_{JS}$ , impeller diameter -  $D/T$ , off-bottom clearance -  $c/D$  and impeller spacing -  $s/D$  respectively.

The second part of the research consisted of determination of the nucleation rate of borax decahydrate in a batch cooling crystallizer at the same stated conditions.

The fundamental thermodynamic driving force of crystallization is given by the change of chemical potential between standing and equilibrium state [26]. Since chemical potential is a quantity that is not easy to measure, for the sake of convenience, the driving force (supersaturation) is expressed as the difference between the measured concentration of the mother liquor,  $c$ , and the equilibrium concentration,  $c^*$ , which was determined from the solubility data [27], [28].

Solubility data of borax decahydrate presented on Fig. 2 (a) was determined in previously published work [29]. Fig. 2 (b) shows a typical example of the supersaturation change during a batch cooling crystallization of borax. In all experiments, supersaturation profiles were similar to the one shown in Fig. 2 (b). At  $t=0$ , crystallizer is filled with a just-saturated solution. As the temperature of the solution decreases, the

solution begins to be supersaturated at a constant rate. The supersaturation increases, reaches a peak and then decreases. Linear increment of supersaturation is a function of salt solubility and cooling rate and it does not depend on mixing conditions. On the other hand, the maximum values of supersaturation ( $\Delta c_{\max}$ ) as well as the subsequent decrease of supersaturation depend on examined mixing parameters. At the maximum value of supersaturation,  $\Delta c_{\max}$ , spontaneous nucleation takes place, thus this value corresponds to the maximum supersaturation e.g. the metastable zone width expressed in terms of concentration.

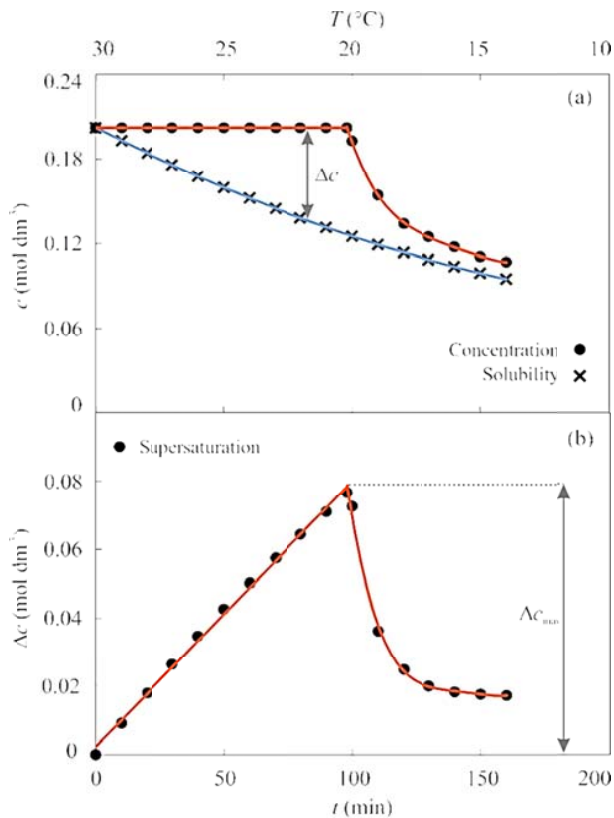


Fig. 2 Concentration and solubility change over process time (a), supersaturation profile (b)

Various mechanisms are proposed to correlate a nucleation process and metastable zone width. In an unseeded batch cooling crystallizer, the primary nucleation mechanism occurs dominantly. In these systems, a homogenous primary nucleation occurs only if a supersaturated solution is free of any particle. On the contrary, a heterogeneous primary nucleation takes place in the presence of foreign particles. The total rate of nucleation,  $N$ , is the sum of the four contributing mechanisms:

$$N = N_{\text{hom}} + N_{\text{het}} + N_{\text{sur}} + N_{\text{att}} \quad (1)$$

where,  $N_{\text{hom}}$ ,  $N_{\text{het}}$ ,  $N_{\text{sur}}$  and  $N_{\text{att}}$  are the rates of homogeneous, heterogeneous, secondary surface nucleation, and the rate of attrition induced secondary nucleation. Kim and Mersmann

[30] proposed that only one contribution is dominant in a given range of supersaturation. They suggested a rapid, simple and indirect method (Fig. 3) to determine the nucleation mechanism in a classical nucleation theory by measuring the degree of supersaturation and solubility at a constant cooling rate.

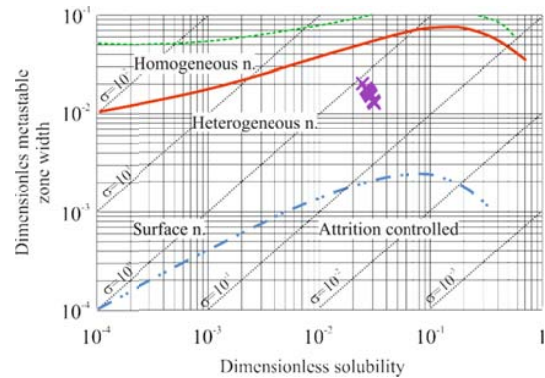


Fig. 3 Mersmann's nucleation criterion

Data obtained in this study were marked on the graph shown in Fig. 3 which presents a relation between dimensionless metastable zone width ( $\Delta c_{\max}/c_c$ ) and dimensionless solubility ( $c^*/c_c$ ), where  $c_c$  is crystal molar density. It was found that the heterogeneous primary nucleation is the dominating mechanism in examined systems (Fig. 3). In that case, nucleation rate can be calculated by [31], [32]:

$$N_{\text{het}} = 0.965 \cdot \varphi_{\text{het}} \frac{D_{\text{AB}}}{d_m^5} \left( \frac{\Delta c_{\max}}{c_c} \right)^{\frac{7}{3}} \cdot \sqrt{f \cdot \ln \frac{c_c}{c^*}} \cdot \exp \left( -1.19 \cdot f \cdot \frac{[\ln(\frac{c_c}{c^*})]^3}{(\nu \cdot \ln S)^2} \right) \quad (2)$$

where,  $\varphi_{\text{het}}$  is the heterogeneity factor,  $D_{\text{AB}}$  is the bulk diffusivity,  $d_m$  is the molecule diameter,  $f$  is the reduction factor (for heterogeneous nucleation  $0 < f < 1$ , it depends on the contact angle between the surface of the foreign particles and the surface of the nucleus),  $c_c$  presents crystal molar density,  $\nu$  number of ions per molecule and  $S$  is relative supersaturation. Calculation was carried out with  $D_{\text{AB}}=10^{-10}$  m<sup>2</sup>/s [33] and  $c_c=4.48$  mol/dm<sup>3</sup> which was valid for estimated parameters of  $\varphi_{\text{het}}=10^{-11}$  and  $f=0.1$  [34].

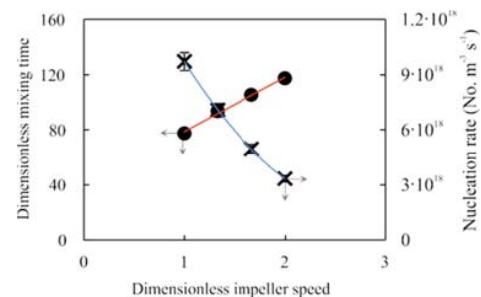


Fig. 4 Dimensionless mixing time and nucleation rate vs. dimensionless impeller speed

Results on Fig. 4 show dependence of dimensionless mixing time ( $N \cdot t_{95}$ ) and nucleation rate on dimensionless impeller speed ( $N/N_{JS}$ ). A decrease in nucleation rate, in nuclei per  $m^3 \cdot s$ , is a consequence of higher level of turbulence, i.e. greater value of the  $N/N_{JS}$  ratio, which caused narrowing of the metastable zone.

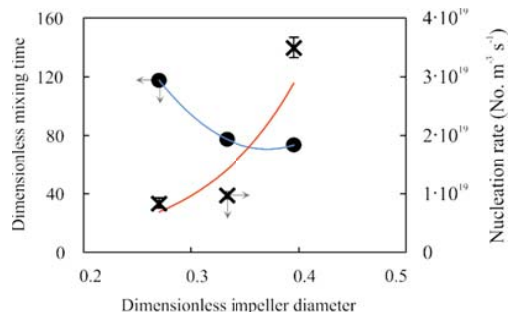


Fig. 5 Dimensionless mixing time and nucleation rate vs. dimensionless impeller diameter

Decrease in the value of mixing time with an increase of impeller diameter ( $D/T$ ) was observed. As is shown in Fig. 5, the values of mixing time show tendency of approaching a constant value. At the same time, the value of nucleation rate is increased. The reason for this lies in the fact that radial flow impellers impose essentially shear stress to the fluid. The larger the impeller more pronounced the shear forces that break stable nuclei in formation are. This postponed nucleation i.e. widened the metastable zone and resulted in the highest nucleation rate in this investigation.

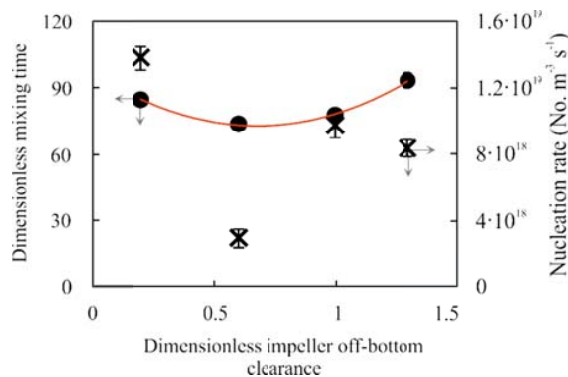


Fig. 6 Dimensionless mixing time and nucleation rate vs. dimensionless impeller off-bottom clearance

Results of the experiments shown in Figs. 4 and 5 were conducted at constant impeller position where  $c/D$  and  $s/D$  equaled 1. However, as several studies have shown [35]–[37], impeller position does matter. Depending on the impeller off-bottom clearance and/or impeller spacing, the overall fluid flow in the vessel can differ greatly. As was presumed, our investigation showed that both mixing time and nucleation rate are influenced by the impeller position as can be seen on Figs. 6 and 7. A parabolic dependence of mixing time on the values of off-bottom clearance has a minimum at  $c/D=0.6$ .

Depending on the values of impeller off-bottom clearance and impeller spacing, Rutherford et al. [38] divided stable flow patterns in multiple impeller systems into three types: parallel, merging, and diverging flow. If a lower impeller is too close to the vessel bottom (in our research this was at  $c/D=0.2$ ), a diverging flow will form. In that case, lower impeller stream follows a path toward and impinges upon the base of the vessel. Practically, it is not able to fully “develop” and its contribution to the overall fluid flow in the vessel is weakened. The value of heterogeneous nucleation rate calculated for  $c/D=0.2$  confirms this, as it is relatively high which was a consequence of the described diverging flow. From  $c/D=0.6$  to 1.3, nucleation rate increases.

Depending on the impeller spacing, an interaction of the fluid flow generated by each impeller can be more or less pronounced. Results shown in Fig. 7 indicate that both mixing time and nucleation rate increase with an increment of impeller spacing.

Among other, two extremes are investigated here. The first one is when impeller spacing equals zero. In that case, two impellers acted like one but with modified geometric characteristics where dimensionless impeller blade width,  $w/D$  was equal to 0.5. This resulted in the lowest value of  $N \cdot t_{95}$  in this part of the investigation. The other extreme is when the two impellers are set so apart (in this case when  $s/D=1.5$ ) that the flows which they generate are completely independent of each other. This resulted in poor mixing in the region between the impellers and the highest value of  $N \cdot t_{95}$  in all examined configurations.

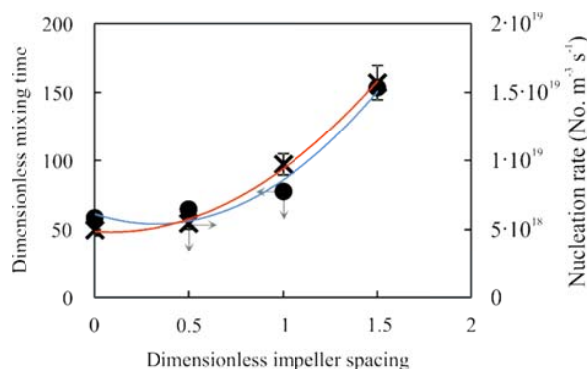


Fig. 7 Dimensionless mixing time and nucleation rate vs. dimensionless impeller spacing

Mixing time measurements showed that merging flow ( $s/D=0$  to  $s/D=1$ ) led to a lower value of dimensionless mixing time compared to the parallel ( $s/D=1.5$ ) and diverging flow patterns ( $c/D=0.2$ ). This is in accordance with the findings of Rutherford et al. [38]. Regarding the values of nucleation rate, an increase with an increment of impeller spacing was observed. At  $s/D=1.5$  the rate of nucleation was among highest ones obtained in this investigation.

The fact that there are no crystals present in the solution prior to nucleation enabled us to investigate if there is a correlation between the values of mixing time and nucleation rate. In Fig. 8, a scatter diagram of nucleation rate against

dimensionless mixing time, along with the values of correlation coefficient -  $r$  is given. It suggests that nucleation rate and  $N \cdot t_{95}$  strongly correlate in systems where  $N/N_{JS}$  and  $s/D$  were investigated. Correlation was shown to be moderate at  $D/T$ ,  $c/D$ . These findings suggest that the nucleation rate is affected by the value of mixing time and in order to produce crystals of desired properties it should be taken into account.

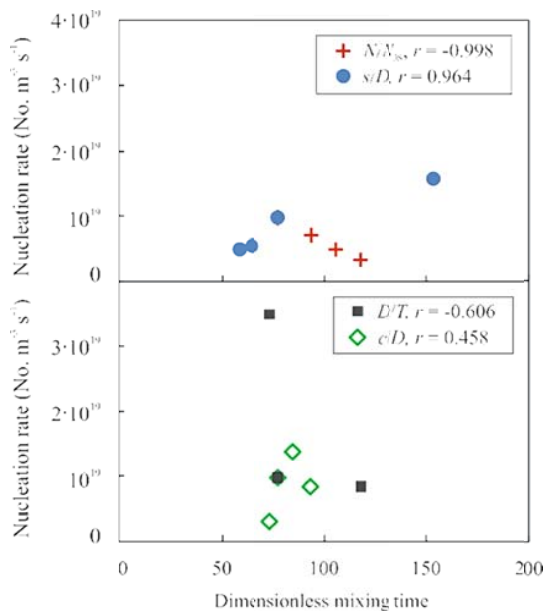


Fig. 8 Scatter diagram of nucleation rate against dimensionless mixing time

TABLE I  
POWER CONSUMPTION VALUES FOR TESTED SYSTEMS

Mixing parameter	$P/m$ (W/kg)
1	3.35
$N/N_{JS}$	1.33
(at $D/T=0.33$ , $c/D, s/D=1$ )	1.67
2	20.56
$D/T$	0.27
(at $N/N_{JS}$ , $c/D, s/D=1$ )	0.33
0.40	2.51
0.2	0.81
$c/D$	0.6
(at $D/T=0.33$ , $N/N_{JS}, s/D=1$ )	1
1.3	7.32
0	2.11
$s/D$	0.5
(at $D/T=0.33$ , $N/N_{JS}, c/D=1$ )	1
1.5	6.16

In this research, the effect of the mixing parameters (impeller speed, size and position) on power consumption was investigated as well. This value represents the energy brought into the system through impellers and it is usually represented as the ratio of power consumed per unit mass -  $P/m$ . Power was calculated using (3)

$$P = 2\pi \cdot N \cdot \tau \quad (3)$$

where  $\tau$  represents torque which was measured continuously.

Results showed that power consumption increased with an increment of  $N/N_{JS}$ . An increase of impeller diameter resulted in lowering of the power consumption. The reason for this lies in the fact that all experiments (except the ones where  $N/N_{JS}$  was tested) were conducted at the values  $N=N_{JS}$ . The larger the impeller the lower impeller speed is required to ensure the state of complete suspension.

Impeller position reflects on the amount of the power consumed as well. It was found that the value of  $P/m$  increases with an increment of both impeller off-bottom clearance and impeller spacing. These results are directly linked to the value of critical impeller speed ( $N_{JS}$ ). The fact is that the speed at which the state of complete suspension is achieved is dependent on the impeller position. Since its value increased with an increment of  $c/D$  and  $s/D$  (as a consequence of the existence of zones of lower mixedness at certain impeller positions), it directly reflected on the values of power consumed per unit mass.

#### IV. CONCLUSIONS

In this paper, a dependence of dimensionless mixing time and nucleation rate of borax decahydrate on mixing parameters (impeller speed, size and position) was found. It suggests that in order to obtain a product of desired properties, a dual impeller crystallizer with specific mixing parameters should be considered. Obviously, different mixing parameters result in different flow patterns, the effect of which (on the crystallization kinetics of borax decahydrate) will be investigated in the future.

#### REFERENCES

- [1] K. Shimizu, H. Nagasawa and K. Takahashi, "Effect of off-Bottom Clearance of a Turbine Type Impeller on Crystal Size Distribution of Aluminum Potassium Sulfate in a Batch Crystallizer", *J. Crystal Growth*, 1995. 154: p. 113-117.
- [2] K. Shimizu, T. Nomura and K. Takahashi, "Crystal Size Distribution of Aluminum Potassium Sulfate in a Batch Crystallizer Equipped with Different Types of Impeller," *J. Crystal Growth*, 1998. 191(1-2): p. 178-184.
- [3] K. Shimizu et al., "Effect of Baffle Geometries on Crystal Size Distribution of Aluminum Potassium Sulfate in a Seeded Batch Crystallizer," *J. Crystal Growth*, 1999. 197(4): p. 921-926.
- [4] L. Marmo et al., "Influence of mixing on the particle size distribution of an organic precipitate," *J. Crystal Growth*, 1996. 166: p. 1027-1034.
- [5] Z. Sha and S. Palosaari, "Mixing and Crystallization in Suspension," *Chem. Eng. Sci.*, 2000. 55: p. 1797-1806.
- [6] E. L. Paul, V. A. Atiemo-Obeng and S. Kresta, *Handbook of Industrial Mixing*, Hoboken, New Jersey: John Wiley and Sons, Inc., 2004, pp. 1027-1029.
- [7] I. Fort and T. Jirout, "A study on blending characteristics of axial flow impellers," *Chem. Proc. Eng.*, 2011. 32 (4): p. 311-319.
- [8] J. Landau and J. Procházka, "Experimental methods for following the homogenation of miscible liquids by rotary mixers," *Collect. Czech. Chem. Commun.*, 1961. 26: p. 1976-1990.
- [9] G. Delaplace et al., "Determination of mixing time by colourimetric diagnosis - Application to a new mixing system," *Exp. Fluids*, 2004. 36: p. 437-443.
- [10] R. Mann et al., "Computational Fluid Mixing for Stirred Vessels - Progress from Seeing to Believing," *Chem. Eng. J. Biochem. Eng. J.*, 1995. 59: p. 39-50.
- [11] O. Visuri, M. Laakkonen and J. Aittamaa, "A digital imaging technique for the analysis of local inhomogeneities from agitated vessels," *Chem. Eng. Technol.*, 2007. 30: p. 1692-1699.

- [12] N. Otomo et al., „A novel measurement technique for mixing time in an aerated stirred vessel,” *J. Chem. Eng. Jpn.*, 2003. 36: p. 66-74.
- [13] W. M. Lu, H. Z. Wu and M. Y. Ju, „Effects of baffle design on the liquid mixing in an aerated stirred tank with standard Rushton turbine impellers,” *Chem. Eng. Sci.*, 1997. 52: p. 3843-3851.
- [14] E. A. Fox and V. E. Gex, „Single-Phase Blending of Liquids,” *AIChE J.*, 1956. 2: p. 539-544.
- [15] I. Houcine, E. Plasari and R. David, “Effects of the Stirred Tank's Design on Power Consumption and Mixing Time in Liquid Phase,” *Chem. Eng. Technol.*, 2000. 23: p. 605-613.
- [16] P. Sayan, S. Titz Sargut and B. Kiran, “Effect of impurities on the microhardness of borax decahydrate,” *Powder Technology*, 2010. 197: p. 254-259.
- [17] W. D. Einkenkel and A. Mersmann, "Erforderliche Drehzahl zum Suspendieren in Rührwerken," *Verfahrenstechnik*, 1977. 11 (2): p. 90-94.
- [18] T. N. Zwietering, "Suspending of Solid Particles in Liquid Agitators," *Chem. Eng. Sci.*, 1958. 8: p. 244-253.
- [19] M. Jahoda et al., “CFD modelling of liquid homogenization in stirred tanks with one and two impellers using large eddy simulation,” *Chem. Eng. Res. Des.*, 2007. 85: p. 616–625.
- [20] O. Sahin, “Effect of Borax on the Crystallization of Boric Acid,” *J. Crystal Growth*, 2002. 236: p. 393-399.
- [21] F. Jones et al., “The Effect Of Calcium Cations on the Precipitation of Barium Sulfate 2: Calcium Ions in the Presence of Organic Additives,” *J. Crystal Growth*, 2004. 270: p. 593-603.
- [22] D. C. Y. Wonh, Z. Jaworski and A. W. Nienow, “Effect of Ion Excess on Particle Size and Morphology During Barium Sulfate Precipitation: An Experimental Study,” *Chem. Eng. Sci.*, 2001. 56: p. 727-734.
- [23] J. C. Givand, A. S. Teja and R. W. Rousseau, “Manipulating Crystallization Variables to Enhance Crystal Purity,” *J. Crystal Growth*, 1999. 198/199: p. 1340-1344.
- [24] S. Ramalingom, J. Podder and S. Narayana Kalkura, “Crystallization and Characterization of Orthorhombic  $\beta$ -  $MgSO_4 \cdot 7H_2O$ ,” *Crys. Res. Technol.*, 2001. 36(12): p. 1357-1364.
- [25] A. Nokhoddchi, N. Bolourtchiana and R. Dinarvand, “Crystal Modification of Phenytoin Using Different Solvents and Crystallization Conditions,” *Int. J. Pharm.*, 2003. 250: p. 85-87.
- [26] A. G. Jones, *Crystallization Process Systems*, London: Butterworth-Heinemann, 2002, pp. 58-141.
- [27] J. W. Mullin, *Crystallization*, 4th ed., Oxford: Butterworth-Heinemann, 2001, pp. 86-403.
- [28] A. Myerson, *Handbook of Industrial Crystallization*, Boston: Butterworth-Heinemann, 2002, pp. 1-218.
- [29] M. Akrap, N. Kuzmanica and J. Prlić-Kardum, “Effect of mixing on the crystal size distribution of borax decahydrate in a batch cooling crystallizer,” *J. Crystal Growth*, 2010. 312(24): p. 3603-3608
- [30] K. J. Kim and A. Mersmann, “Estimation of Metastable Zone Width in Different Nucleation Processes,” *Chem. Eng. Sci.*, 2001. 56(7): p. 2315-2324.
- [31] A. Schubert and A. Mersman, “Determination of Heterogeneous Nucleation Rates,” *Trans. Inst. Chem. Eng.*, 1996. A 74(1): p. 816-821.
- [32] A. Mersmann, “Supersaturation and Nucleation,” *Trans IChemE*, 1996. 74(A): p. 812-819.
- [33] A. Mersmann, „General prediction of statistically mean growth rates of a crystal collective,” *J. Crystal Growth*, 1995. 147: p. 181-193.
- [34] Y. H. Cheon, K. J. Kim and S. H. Kim, „A study on crystallization kinetics of pentaerythritol in a batch cooling crystallizer,” *Chem. Eng. Sci.*, 2005. 60: p. 4791-4802.
- [35] R. Kuboi and A. W. Nienow, “The power drawn by dual impeller systems under gassed and ungassed conditions,” In: *Proc. 4th Eur. Conf. Mix.*, Noordwijkerhout, the Netherlands, 1982, pp. 247.
- [36] Z. X. Weng, “The effect of the distance between multiple impellers in the turbulent tank,” *Chem. Eng.*, 1983. 6: p. 1–6.
- [37] V. Mishra and J. Joshi, “Flow generated by a disc turbine. IV: Multiple impellers,” *Chem. Eng. Res. Des.*, 1994. 72: p. 657-668.
- [38] K. Rutherford et al., “Hydrodynamic characteristics of dual Rushton impeller stirred vessels,” *AIChE J.*, 1996. 42: p. 332–346.